

Nonconventional Host–Guest Cubic Assembly Based on γ -Cyclodextrin and Keggin-type Polyoxometalate

Zhan-Guo Jiang,# Wei-Tao Mao,# Dan-Ping Huang, Yu Wang, Xiao-Juan Wang, and Cai-Hong Zhan*

Table of Contents

S1 Materials	2
S2 General Experimental Section	2
Powder X-ray Diffraction (PXRD)	2
Fourier Transform Infrared Spectroscopy (FTIR)	2
Elemental Analyses (EA)	2
Thermogravimetric Analyses (TGA)	2
Nuclear Magnetic Resonance spectra (NMR)	2
Cyclic voltammetry (CV)	3
Electrospray Ionization Mass Spectrometry (ESI-MS)	3
Single-crystal X-ray diffraction (SCXRD)	3
S3. Synthesis and Experimental Section	4
Synthesis of Co-POM-CD (1)	4
Synthesis of Cu-POM-CD (2)	4
S4. Crystal data and structure refinement	4
S5. Crystal structures	6
S6 Electrospray Ionization Mass Spectrometry (ESI-MS)	9
S7 ³¹P NMR spectra	12
S8 ¹³C NMR	13
S9 ¹H NMR spectra	14
S10 Fourier Transform Infrared Spectroscopy (FTIR)	14
S11 Powder X-ray diffraction (PXRD)	17
S12 Thermogravimetric analyses (TGA)	18
S13 Cyclic voltammetry (CV)	19
S14 Reference	19
S15 Tables for bond lengths	20

S1 Materials

All starting materials and reagents were purchased from commercial suppliers and used without further purification. γ -Cyclodextrins (98%) and $\text{Co}(\text{NO}_3)_2 \cdot 6\text{H}_2\text{O}$ (99.99% metals basis) were purchased from Aladdin. $\text{Na}_3\text{PW}_{12}\text{O}_{40} \cdot \text{XH}_2\text{O}$ (98%) was purchased from Energy, and $\text{CuSO}_4 \cdot 5\text{H}_2\text{O}$ (AR) as well as concentrated hydrochloric acid (AR) were purchased from Sinopharm Chemical Reagent Co., Ltd., China.

S2 General Experimental Section

Powder X-ray Diffraction (PXRD)

Powder XRD patterns were obtained using a Bruker D8 Advance X-ray diffractometer with (λ ($\text{CuK}\alpha$) = 1.5405 Å) radiation.

Fourier Transform Infrared Spectroscopy (FTIR)

The materials were recorded on KBr disk using a Nicolet NEXUS 670 spectrometer between 400 and 4000 cm^{-1} .

Elemental Analyses (EA)

C H microanalyses were performed on a Perkin-Elmer 240C elemental analyser, and ICP-OES analyses were carried out on a PerkinElmer Optima 8300 optical emission spectrometer.

Thermogravimetric Analyses (TGA)

They were carried out on a TA Instruments STA499 F5 thermobalance with a 100 $\text{mL} \cdot \text{min}^{-1}$ flow of nitrogen; the temperature was ramped from 20 °C to 800 °C at a rate of 5 °C $\cdot \text{min}^{-1}$.

Nuclear Magnetic Resonance spectra (NMR)

The NMR spectra were recorded on a Bruker Advance III 600 MHz instrument at room temperature, using 5 mm tubes for ^1H , ^{13}C and ^{31}P . Generally, ~20 mg of sample was dissolved in 600 μl of solvent, before transferring to an NMR tube.

Samples and γ -CD were respectively dissolved in D_2O , and $\text{Na}_3\text{PW}_{12}\text{O}_{40} \cdot \text{XH}_2\text{O}$ was

dissolved in ultrapure water. The hydrogen and carbon nuclear magnetic spectra of samples were compared with γ -CD and phosphorus spectra was compared with $\text{Na}_3\text{PW}_{12}\text{O}_{40}\cdot\text{XH}_2\text{O}$.

Cyclic voltammetry (CV)

Cyclic voltammetry (CV) experiments were carried out at room temperature in H_2O with a VersaSTAT 3F instrument (Advanced Measurement Technology Inc.). All CV experiments were performed using a glassy carbon (GC) electrode with a diameter of 3 mm as the working electrode. The electrode surface was polished routinely with 0.05 μm alumina–water slurry on a felt surface immediately before use. The counter electrode was a Pt wire and the reference electrode was a saturated calomel electrode (SCE) electrode. After $\text{Na}_3\text{PW}_{12}\text{O}_{40}$ was dissolved in water, using hydrochloric acid to adjust the pH of the solution until it achieved 1.0. And then under 298 K, scan rate 0.1 V s^{-1} of a 0.1 M aqueous solution of the $[\text{PW}_{12}\text{O}_{40}]^{3-}$ trianion in the presence of increasing amounts of γ -CD from 0.02 to 0.2 M.

Electrospray Ionization Mass Spectrometry (ESI-MS)

Mass spectra were recorded on an Agilent 6224 (Agilent Technologies, USA) ESI-TOF-MS spectrometer. Sample solutions are infused by a syringe pump at 4 $\mu\text{L}/\text{min}$. Data were acquired using the following settings: ESI capillary voltage was set at 3500 V (–) ion mode and fragmentor at 200 V. The liquid nebulizer was set to 15 psig and the nitrogen drying gas was set to a flow rate of 4 L/min. Drying gas temperature was maintained at 15°C. The reported m/z values represent monoisotopic mass of the most abundant peak within the isotope pattern.

Single-crystal X-ray diffraction (SCXRD)

A suitable crystal of Co-POM-CD and Cu-POM-CD were mounted in a Hampton cryoloop with Paratone® N oil cryoprotectant. Intensity data collections were carried out at $T = 120(2)$ K with a Bruker D8 VENTURE diffractometer equipped with a PHOTON 100 CMOS bidimensional detector using a high brilliance $\text{I}\mu\text{S}$ microfocus X-ray Mo Ka monochromatized radiation ($\lambda = 0.71073$ Å). The structures were solved by intrinsic phasing methods and refined by full-matrix least squares using the SHELX-TL package.¹ All atoms were refined with anisotropic thermal parameters except for solvent molecules and disorderly few atoms on CD. Hydrogen atoms on water and on hydroxyl groups on CDs are not identified. Positions of the remaining hydrogen atoms belonging to the CDs were calculated and refined isotropically using the gliding mode. Further details about of the crystal structure determinations may be

obtained free of charge via the Internet at <http://pubs.acs.org>. CCDC 1978774-1978775. Crystallographic data for single-crystal X-ray diffraction studies are summarized in Table S1.

S3. Synthesis and Experimental Section

Synthesis of Co-POM-CD (1)

In a 10 ml beaker, 0.1768 g (0.06 mmol) of $\text{Na}_3\text{PW}_{12}\text{O}_{40}\cdot\text{XH}_2\text{O}$ was dissolved in 6 ml of ultrapure water, then HCl was added to the mixture until the solution pH = 1, then 0.085 g (0.065 mmol) of γ -CD and 0.1746 g (0.6 mmol) $\text{Co}(\text{NO}_3)_2\cdot 6\text{H}_2\text{O}$ were added successively upon stirring at room temperature. The clear pink solution was allowed to evaporate in an open vial at room temperature. The block-shaped pink crystals of **1** started to appear after one day, which was collected by filtration and air-dried. Yield: 76.6 % based on $\text{Na}_3\text{PW}_{12}\text{O}_{40}$. FT-IR spectrum of **1** is given in Figure S12. $\text{NaCo}(\text{H}_2\text{O})_6\text{H}_6(\text{PW}_{12}\text{O}_{40})_3(\text{C}_{48}\text{H}_{80}\text{O}_{40})_3(\text{H}_2\text{O})_{60}$. Elemental analysis: Calc. (found): H 2.8 (2.5); C 12.7 (12.5); W 48.7 (45.5); Na 0.17 (0.27); Co 0.43 (0.34). TGA (Figure S14) showed a weight loss of 7.8 % in the 20-120 °C temperature range corresponding to the 60 hydration water filled the holes in the compound.

Synthesis of Cu-POM-CD (2)

In a 10 ml beaker, 0.1768 g (0.06 mmol) of $\text{Na}_3\text{PW}_{12}\text{O}_{40}\cdot\text{XH}_2\text{O}$ was dissolved in 6 ml of ultrapure water, then HCl was added to the mixture until the solution pH = 1. Then 0.085 g (0.065 mmol) of γ -CD and 0.1498 g (0.6 mmol) $\text{CuSO}_4\cdot 5\text{H}_2\text{O}$ were added successively upon stirring at room temperature. The clear blue solution was allowed to evaporate in an open penicillin bottle at room temperature. The block-shaped pale blue crystals of **2** started to appear after two days, which was collected by filtration and air-dried. Yield 70.2 % based on $\text{Na}_3\text{PW}_{12}\text{O}_{40}$. FT-IR spectrum of **2** is given in Figure S12. $\text{NaCu}(\text{H}_2\text{O})_6\text{H}_6(\text{PW}_{12}\text{O}_{40})_3(\text{C}_{48}\text{H}_{80}\text{O}_{40})_3(\text{H}_2\text{O})_{49}$. Elemental analysis: Calc. (found): H 2.6 (2.9); C 12.5 (12.2); W 47.9 (48.5); Na 0.17 (0.11); Cu 0.46 (0.51). TGA (Figure S14) showed a weight loss of 6.5 % in the 20-120 °C temperature range corresponding to the 49 hydration water filled the holes in the compound.

In the experiment, various ratio of CD with POM (CD:POM = 1:1 to 1:5 and POM:CD = 1:1 to 1:5) and pH from 1 to 6 with the interval of 0.5 were conducted. The result shows that only in pH = 1/1.5 and CD:POM = 1:1 with the addition of transition metal cations ($\text{Co}^{2+}/\text{Cu}^{2+}$), the super cubic structures were constructed.

S4. Crystal data and structure refinement

Table S1. Crystal data and structure refinement for **Co-POM-CD** and **Cu-POM-CD**.

Compound	Co-POM-CD	Cu-POM-CD
Empirical formula	$C_{144}H_{165}CoNaO_{252}P_3W_{36}$	$C_{144}H_{165}CuNaO_{250}P_3W_{36}$
Formula weight	12721.18	12693.79
Temperature/K	120	120
Crystal system	cubic	cubic
Space group	I23	I23
a/Å	41.7665(8)	41.6063(14)
b/Å	41.7665(8)	41.6063(14)
c/Å	41.7665(8)	41.6063(14)
$\alpha/^\circ$	90	90
$\beta/^\circ$	90	90
$\gamma/^\circ$	90	90
Volume/Å ³	72859(4)	72024(7)
Z	8	8
ρ_{calc}/cm^3	2.319	2.341
μ/mm^{-1}	11.473	11.618
F(000)	46336	46224
Crystal size/mm ³	0.2 × 0.2 × 0.2	0.2 × 0.2 × 0.2
Radiation	MoK α ($\lambda = 0.71073$)	MoK α ($\lambda = 0.71073$)
2 θ range for data collection / °	4.138 to 54.968	4.154 to 54.972
Index ranges	-35 ≤ h ≤ 54, -54 ≤ k ≤ 54, -53 ≤ l ≤ 47	-45 ≤ h ≤ 50, -52 ≤ k ≤ 52, -54 ≤ l ≤ 54
Reflections collected	316581	268668
Independent reflections	27861 [Rint = 0.0718, Rsigma = 0.0354]	27556 [Rint = 0.0548, Rsigma = 0.0312]
Data/restraints/parameters	27861/0/1313	27556/42/1284
Goodness-of-fit on F ²	1.046	1.034
Final R indexes [I ≥ 2 σ (I)]	R1 = 0.0374, wR2 = 0.0999	R1 = 0.0327, wR2 = 0.0912
Final R indexes [all]	R1 = 0.0433, wR2 = 0.1043	R1 = 0.0365, wR2 = 0.0934

data]

Largest	diff.	3.18/-1.42	2.58/-1.30
peak/hole			
/ e Å ⁻³			
Flack parameter		0.014(3)	0.012(3)

S5. Crystal structures

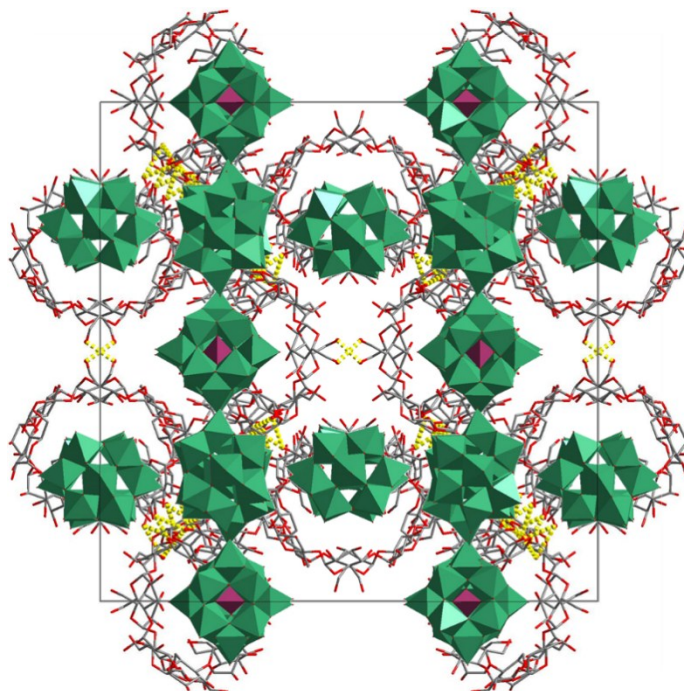


Figure S1 The 3D array of Compounds consisted of (POM @ γ -CD) Second Building Units (SBUs) by hydrogen bonds.

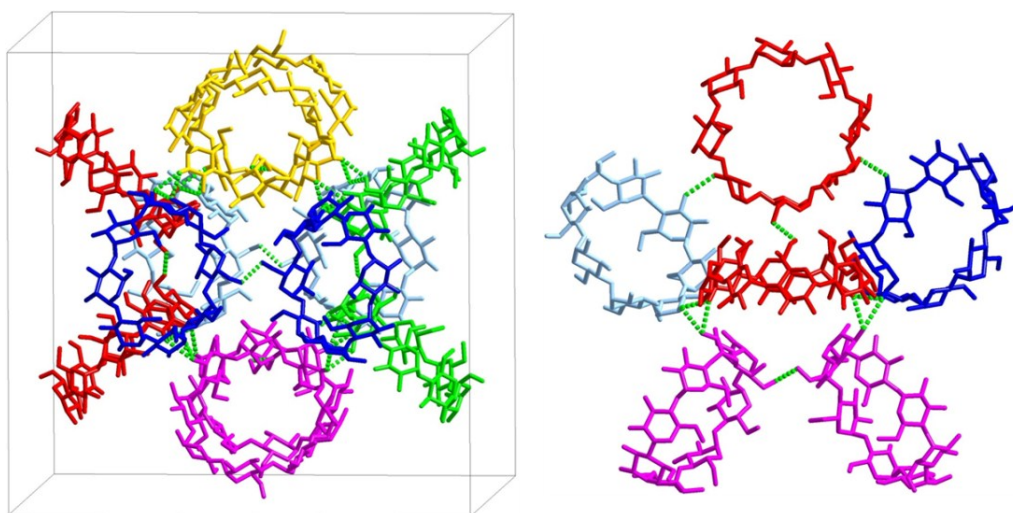


Figure S2 The inner (γ -CD)₁₂ cube is linked by the hydrogen bonds (left), and each symmetrically equivalent γ -CD collects five adjacent γ -CDs (right).

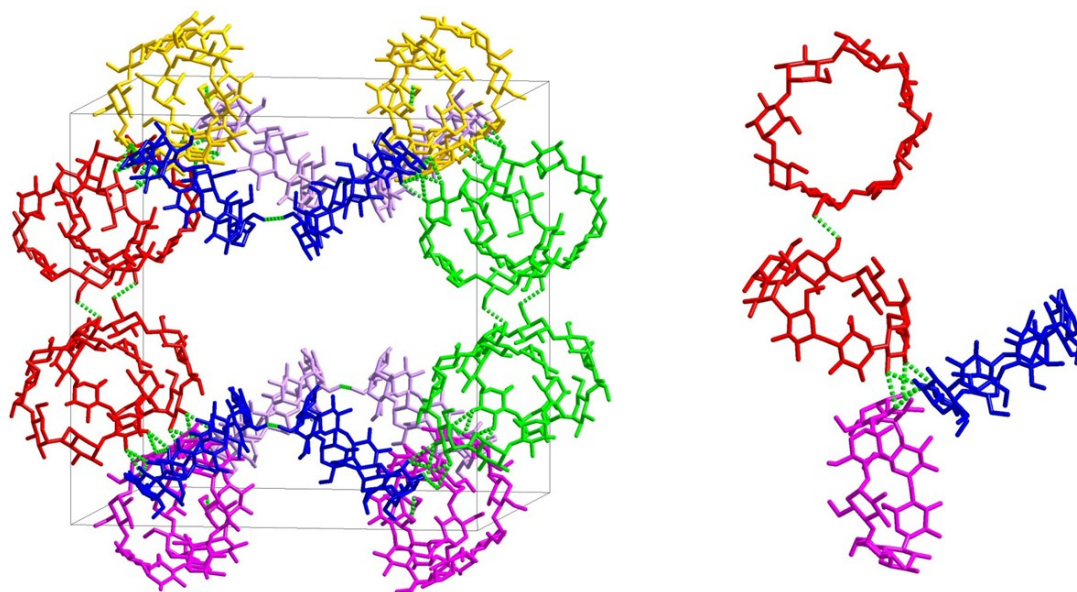


Figure S3 The outer (γ -CD)₁₂ cube is linked by the hydrogen bonds (left), and each symmetrically equivalent γ -CD collects three adjacent γ -CDs (right).

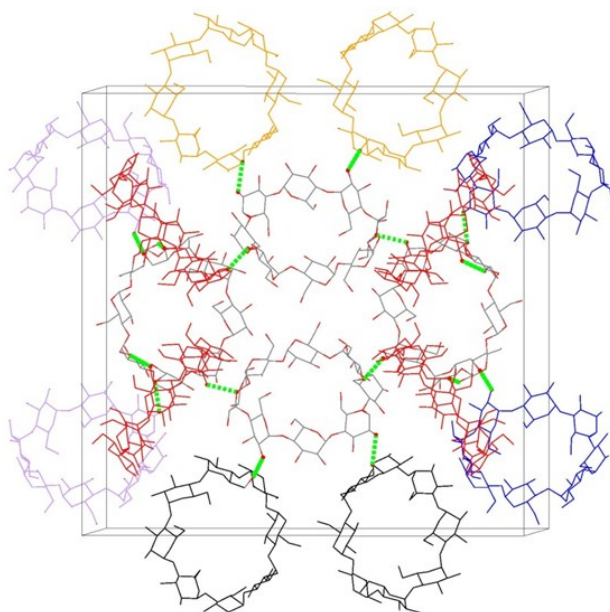


Figure S4 Each inner cubic γ -CD links five outer γ -CD tori by the hydrogen bonds.

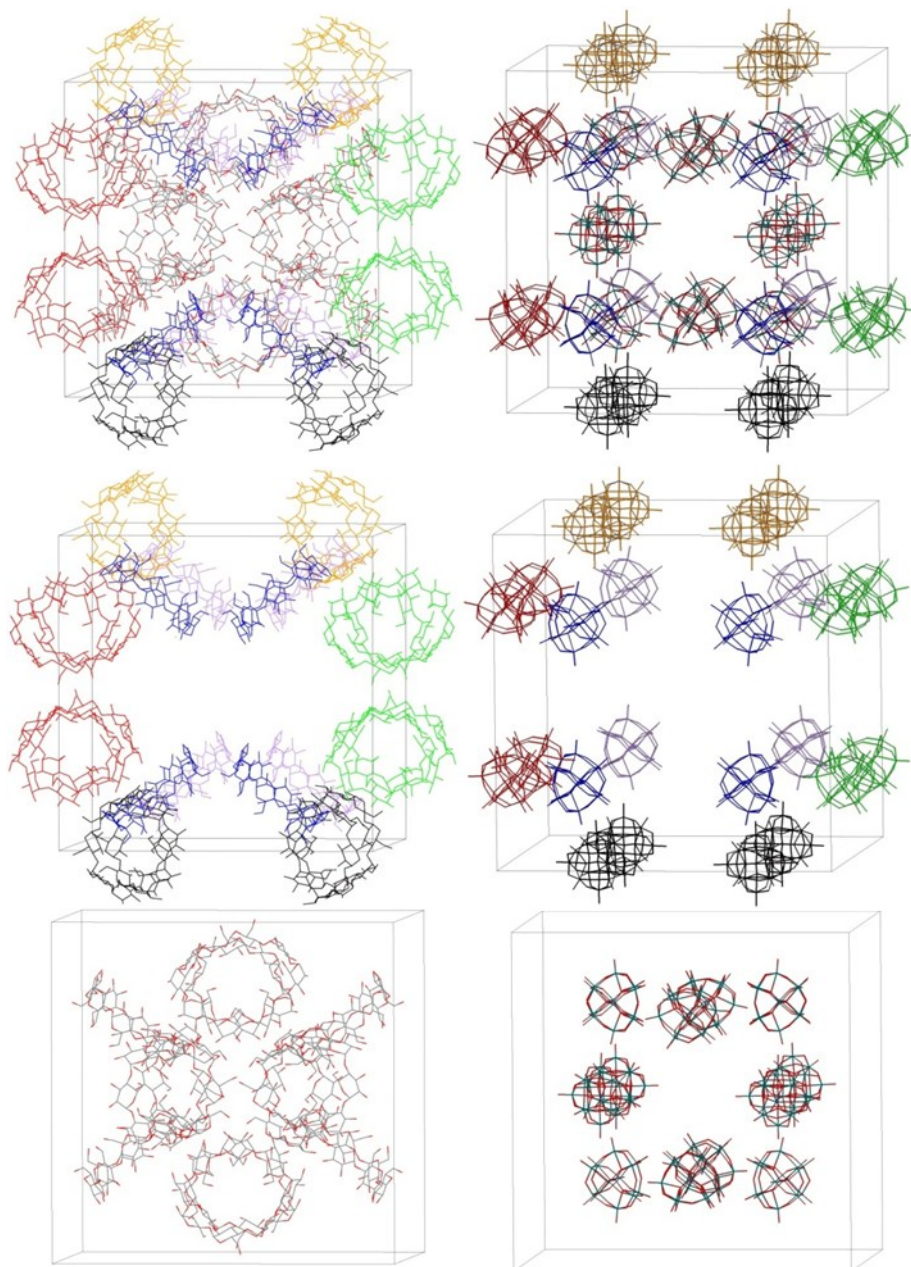


Figure S5 The array of γ -CD (left) and POM (right) in a cell respectively.

Top: the complete $(\gamma\text{-CD})_{36}$ and $(\text{POM})_{36}$. Middle: the outer $(\gamma\text{-CD})_{24}$ and $(\text{POM})_{24}$. Bottom: the inner $(\gamma\text{-CD})_{12}$ and $(\text{POM})_{12}$.

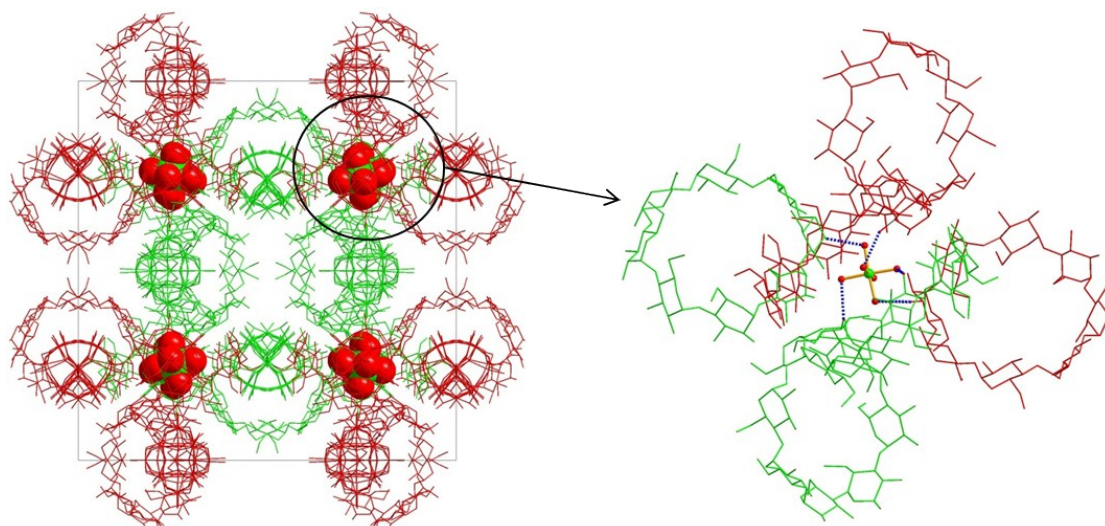


Figure S6 The disordered $[\text{Co/Cu}(\text{H}_2\text{O})_6]^{2+}$ ions bridge the outer (POM @ γ -CD)₂₄ cage and the inner (POM @ γ -CD)₁₂ cage by hydrogen bonding.

S6 Electrospray Ionization Mass Spectrometry (ESI-MS)

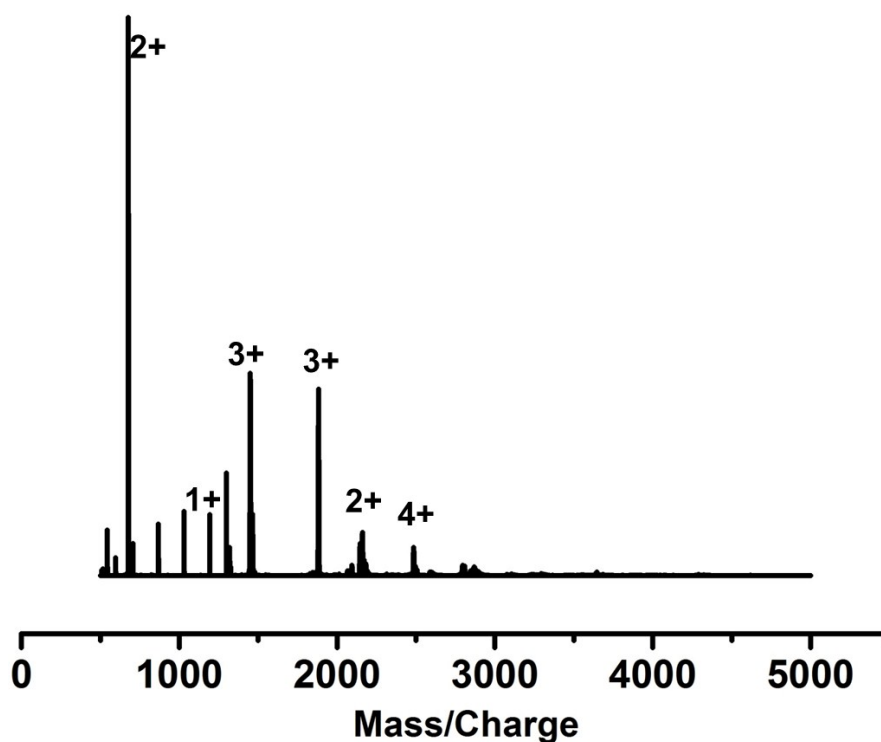


Figure S7 Positive-ion ESI-MS of compound **1** dissolved in $\text{CH}_3\text{CN}/\text{H}_2\text{O}$.

See table S2 below for detailed peak assignments.

Table S2 Selected mass spectrometry peak assignments for compound 1.

m/z (obs)	z	Assignment	m/z (calc)
677.7	2+	[Co-CD]	677.7
1297.4	1+	[H-CD]	1297.4
1450.1	3+	[Co ₃ -POM-CD]	1450.1
1463.8	3+	[Co ₃ -POM-CD·CH ₃ CN]	1463.8
1882.6	3+	[Co ₃ -POM-CD ₂]	1882.6
2146.3	2+	[Co ₂ -HPOM-CD]	2146.3
2158.8	2+	[Co-H ₃ POM-CD·(CH ₃ CN) ₂]	2158.8
2484.8	4+	[Co ₅ -POM ₂ -CD ₃]	2484.8

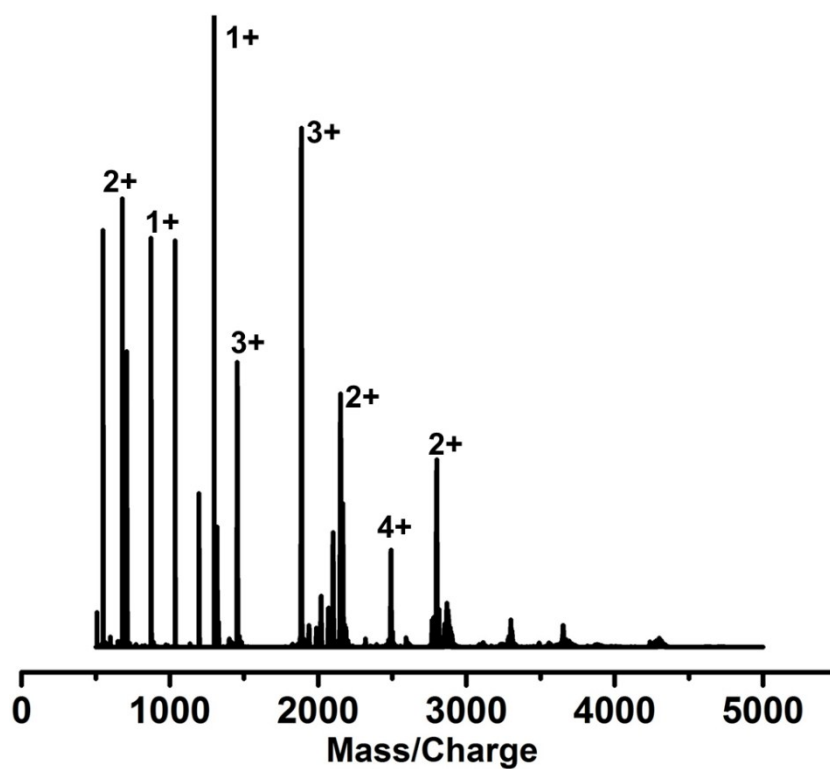


Figure S8 Positive-ion ESI-MS of compound 2 dissolved in CH₃CN/H₂O.

See table S3 below for detailed peak assignments.

Table S3 Selected mass spectrometry peak assignments for compound **2**.

m/z (obs)	z	Assignment	m/z (calc)
679.7	2+	[Cu-CD]	679.7
1297.4	1+	[H-CD]	1297.4
1454.5	3+	[Cu ₃ -POM-CD]	1454.5
1886.9	3+	[Cu ₃ -POM-CD ₂]	1886.9
2150.2	2+	[Cu ₂ -HPOM-CD]	2150.2
2490.8	4+	[Cu ₅ -POM ₂ -CD ₃]	2490.8
2798.9	2+	[Cu ₂ -HPOM-CD ₂]	2798.9

S7 ^{31}P NMR spectra

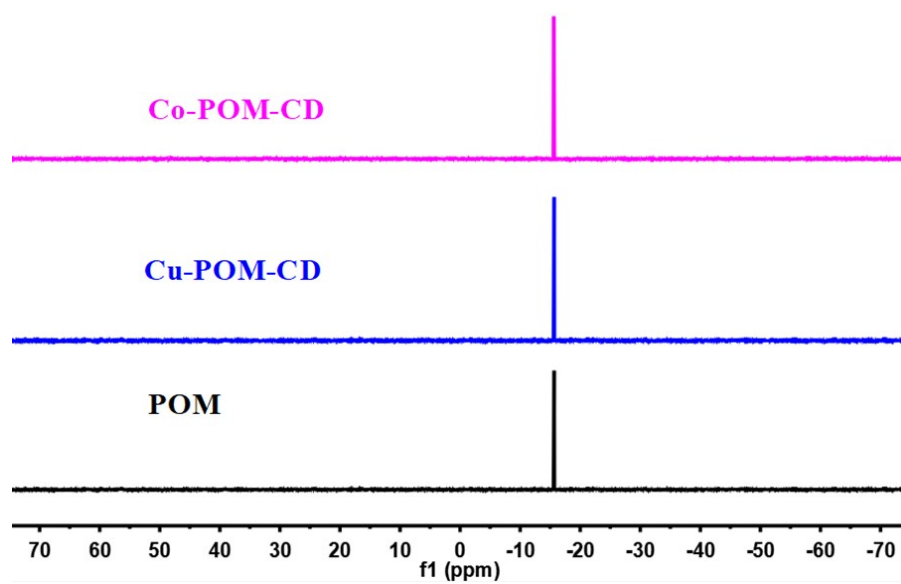


Figure S9 ^{31}P NMR spectra of POM in D_2O solutions, compound **1** (pink) and compound **2** (blue).

S8 ^{13}C NMR

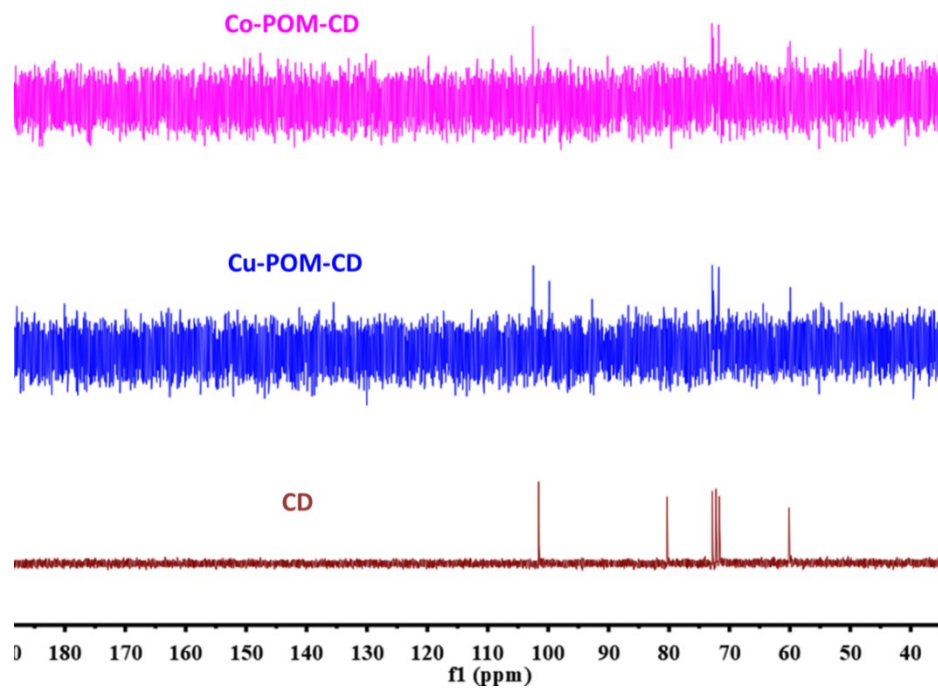


Figure S10 ^{13}C NMR spectra of CD in D_2O solutions, compound **1** (pink) and compound **2** (blue).

S9 ^1H NMR spectra

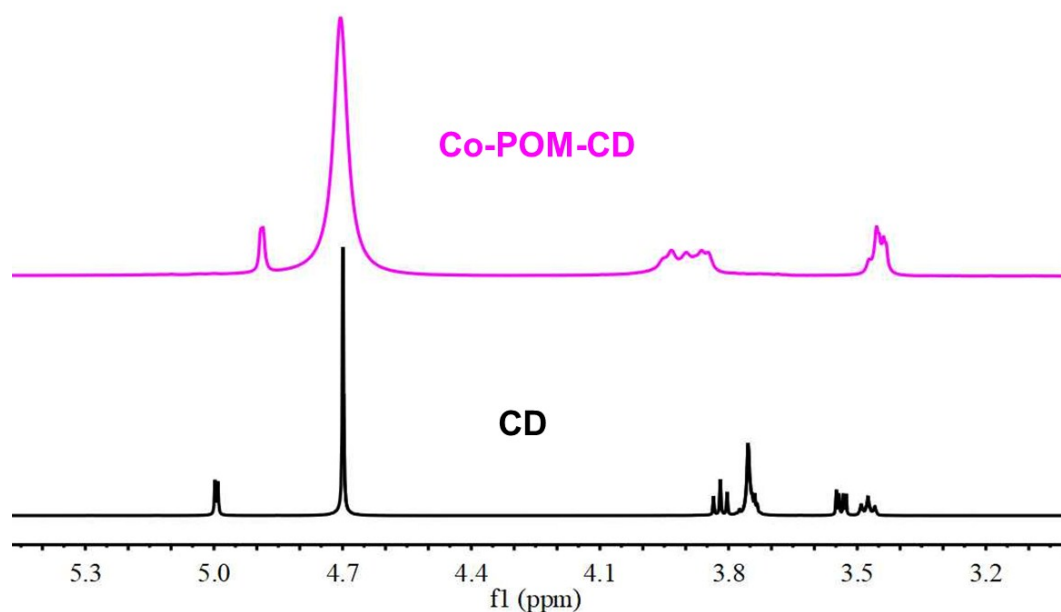


Figure S11 ^1H NMR spectra of bare CD (black) and compound **1** (pink) in D_2O solutions.

S10 Fourier Transform Infrared Spectroscopy (FTIR)

Both characteristic peaks of POM and CD in Co-POM-CD and Cu-POM-CD were shown in the FT-IR spectra.

There are very obvious and apparent signals stretching between 500 and 800 cm^{-1} . Tungstate POMs characteristically exhibit this signal as it corresponds to the W-O-W bridges generally present in these structures.

Also of note is the peak at 955.2 cm^{-1} . This is also characteristic of

tungstate POMs and corresponds to the double bonds between tungsten atoms and terminal oxo-ligands. Beyond these characteristic stretching frequencies common to many POMs, it becomes very difficult to meaningfully assign specific signals to specific parts of the structure due to the highly connected nature of these molecules altering the degrees of freedom available to individual atoms and groups in ways that are not easy to predict. However, there is one more signal that could feasibly be assigned. Broad peaks around 3400 cm^{-1} are characteristic of O-H bonds in hydroxyl groups in water molecules.

On the other hand, the cyclodextrin has strong absorption peak of O-H bonds located at around 3400 cm^{-1} . The band centered at around 2930 cm^{-1} belongs to the asymmetrical stretching vibration of C-H bonds. While the band at around 1640 cm^{-1} originates from the C-C stretching of polysaccharides. The peaks occur in the region from 1470 to 1180 cm^{-1} correspond to the C-H bending vibrations while the band located between $1150\sim 1000\text{ cm}^{-1}$ is characteristic of the symmetrical stretching of glycosidic C-O-C and C-O bonds in polysaccharides.

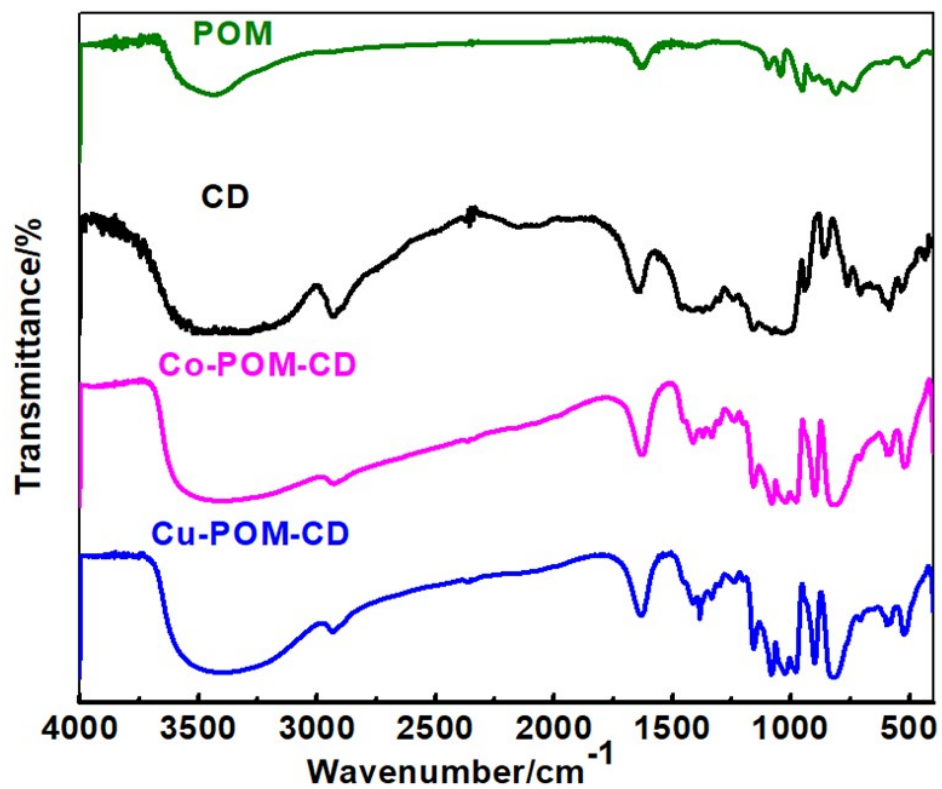


Figure S12 FT-IR spectra of POM, CD, compound 1 and compound 2.

S11 Powder X-ray diffraction (PXRD)

The Powder X-ray diffraction (PXRD) patterns for Co-POM-CD and Cu-POM-CD can be compared with the simulated pattern obtained from the X-ray single-crystal diffraction analysis. Their peak positions are in good agreement with each other, indicating the phase purity of the product. The differences in intensity may be due to the preferred orientation of the powder sample.

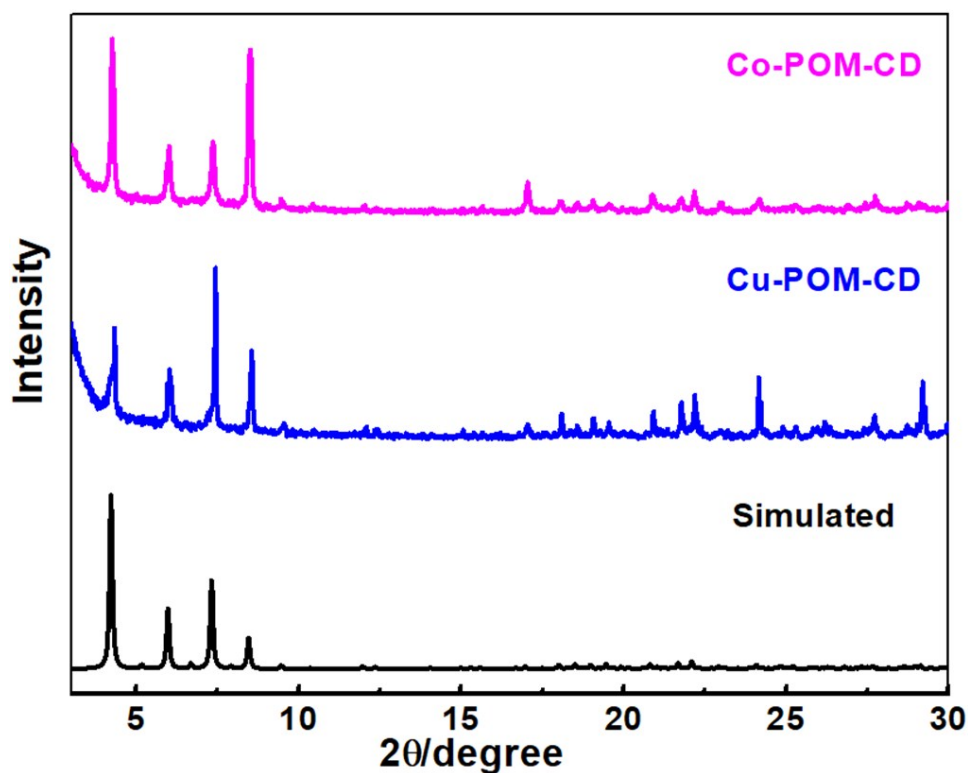


Figure S13 Experimental (pink, compound 1; blue, compound 2) and simulated (black) PXRD patterns.

S12 Thermogravimetric analyses (TGA)

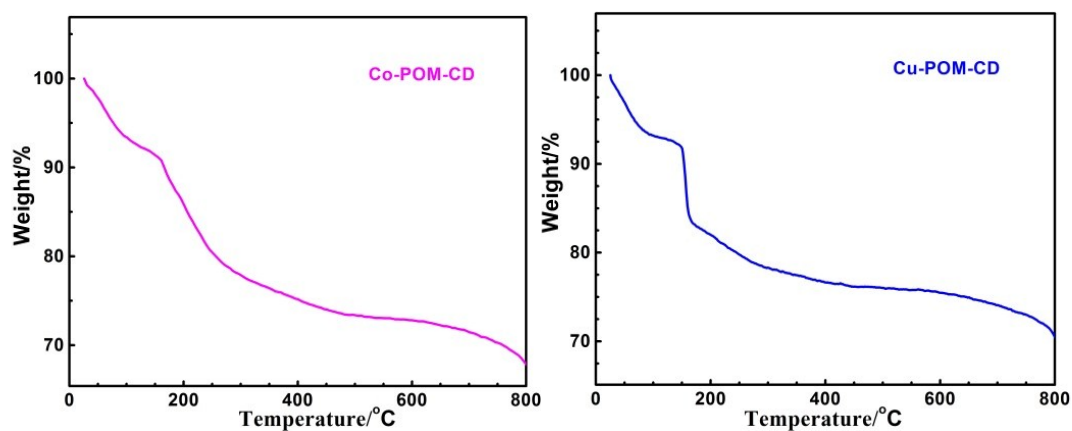


Figure S14 The TGA curves of compound **1** (pink) and compound **2** (blue). TGA of **1** shows a weight loss of 7.8 % in the 20-120°C corresponding to the 60 free water in **1**. TGA of **2** shows a weight loss of 6.5 % in the 20-120°C corresponding to the 49 free water in **2**.

S13 Cyclic voltammetry (CV)

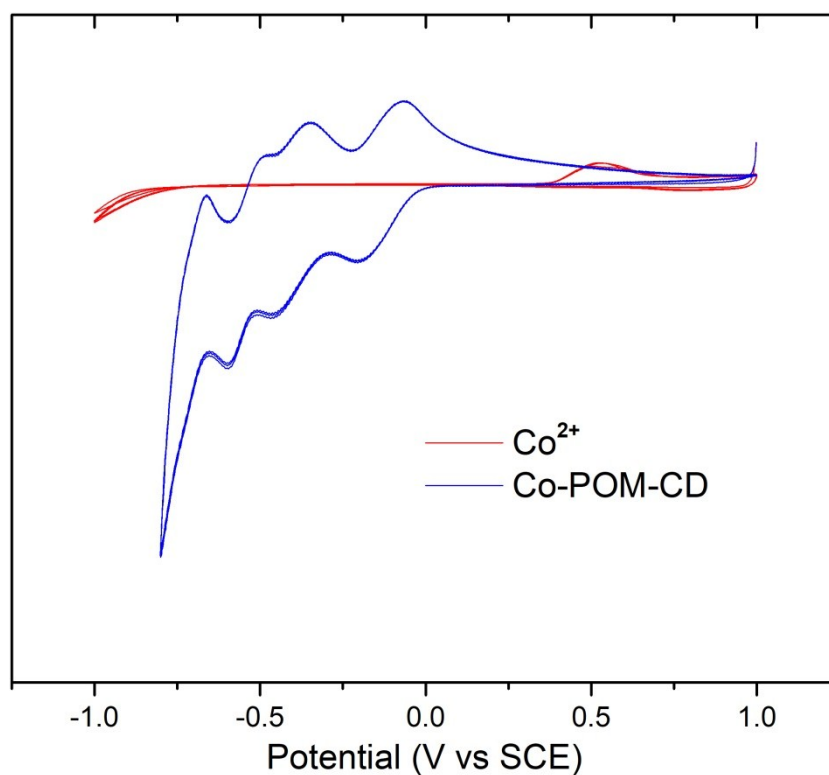


Figure S15 Cyclic voltammograms (298 K, scan rate 100 mV s⁻¹) of Co^{2+} and compound **1** for 3 cycles.

S14 Reference

- 1 Sheldrick, G. M. *Acta Cryst. A* **2008**, 64, 112.

S15 Tables for bond lengths

Table S4. Bond lengths (Å) for Co-POM-CD

W001-O0AA	1.700(11)	W001-O19	1.883(11)
W001-O5	1.898(14)	W001-O1AA	1.939(13)
W001-O11	1.948(12)	W001-O14	2.433(10)
W00A-O52	1.692(13)	W00A-O29	1.875(12)
W00A-O24	1.891(12)	W00A-O19	1.910(11)
W00A-O6B	1.933(11)	W00A-O57	2.432(10)
W00B-O216	1.673(12)	W00B-O100	1.894(11)
W00B-O27	1.896(12)	W00B-O54	1.918(12)
W00B-O77	1.933(12)	W00B-O45	2.439(11)
W00C-O8	1.706(11)	W00C-O1AA	1.864(13)
W00C-O29	1.915(12)	W00C-O49	1.928(12)
W00C-O30	1.951(11)	W00C-O28	2.446(10)
W002-O7	1.672(10)	W002-O96	1.881(11)
W002-O34	1.884(11)	W002-O9	1.905(12)
W002-O49	1.928(12)	W002-O28	2.441(11)
W003-O66	1.700(12)	W003-O42	1.890(10)
W003-O34	1.900(11)	W003-O18	1.904(12)
W003-O77	1.927(11)	W003-O45	2.442(11)
W004-O91A	1.709(11)	W004-O27	1.882(12)
W004-O3	1.898(11)	W004-O91B	1.902(11)
W004-O6B	1.917(12)	W004-O57	2.430(10)
W005-O2AA	1.684(12)	W005-O71	1.889(11)
W005-O30	1.899(12)	W005-O21	1.923(11)
W005-O9	1.941(12)	W005-O28	2.443(9)
W006-O4	1.692(12)	W006-O100	1.889(11)
W006-O3	1.897(12)	W006-O62	1.921(12)
W006-O5	1.960(14)	W006-O14	2.415(10)
W007-O50	1.687(12)	W007-O15	1.887(12)
W007-O71	1.904(11)	W007-O91B	1.919(11)
W007-O24	1.938(12)	W007-O57	2.436(10)
W008-O36	1.700(12)	W008-O11	1.897(12)
W008-O96	1.903(11)	W008-O42	1.916(10)
W008-O62	1.946(11)	W008-O14	2.448(10)
W009-O6A	1.673(10)	W009-O21	1.868(11)
W009-O15	1.898(11)	W009-O54	1.906(12)
W009-O18	1.907(12)	W009-O45	2.430(10)
Co1-O93	2.109(11)	Co1-O217	2.116(14)
P2-O28	1.530(10)	P2-O45	1.535(11)

P2-O57	1.537(10)	P2-O14	1.548(10)
O1-C209	1.35(2)	O1-C17	1.39(3)
O2-C35	1.38(3)	O2-C213	1.48(2)
O6-C23	1.37(3)	O10-C2	1.46(3)
O90-C21	1.32(3)	O90-C24	1.34(3)
O92-C35	1.36(3)	O92-C31	1.41(3)
O94-C7	1.41(3)	O94-C11	1.45(3)
O95-C6	1.41(2)	O95-C187	1.48(3)
O97-C183	1.40(3)	O97-C13	1.42(2)
O98-C185	1.37(2)	O98-C184	1.46(2)
O99-C206	1.44(3)	O99-C32	1.47(3)
O101-C39	1.35(3)	O101-C206	1.46(3)
O102-C182	1.40(3)	O105-C4	1.41(2)
O105-C6	1.41(2)	O106-C7	1.38(2)
O106-C3	1.40(2)	O107-C13	1.40(2)
O107-C10	1.51(2)	O113-C33	1.44(3)
O114-C30	1.46(3)	O115-C14	1.44(2)
O116-C12	1.43(3)	O117-C16	1.44(2)
O121-C36	1.47(4)	O131-C20	1.42(3)
O131-C185	1.49(3)	O133-C18	1.42(3)
O138-C29	1.34(3)	O144-C214	1.39(4)
O145-C25	1.45(3)	O147-C19	1.39(3)
O148-C41	1.54(4)	O149-C8	1.33(3)
O152-C9	1.42(3)	O154-C1	1.42(3)
O155-C5	1.39(4)	O159-C26	1.30(4)
O164-C15	1.39(2)	O166-C208	1.43(3)
O210-C40	1.46(4)	O210-C209	1.42(3)
O211-C28	1.60(4)	O211-C24	1.41(4)
C1-C6	1.53(3)	O212-C37	1.40(3)
C7-C8	1.65(4)	C1-C2	1.54(3)
C8-C9	1.55(4)	C2-C3	1.48(3)
C9-C10	1.58(3)	C3-C4	1.53(3)
C10-C11	1.52(3)	C4-C5	1.59(3)
C11-C12	1.53(3)	C16-C17	1.57(3)
C13-C14	1.53(3)	C17-C20	1.60(3)
C14-C15	1.48(3)	C18-C185	1.65(3)
C15-C184	1.51(3)	C19-C20	1.54(4)
C16-C18	1.49(3)	C21-C23	1.54(3)
C21-C40	1.60(4)	C25-C26	1.70(4)
C23-C182	1.65(3)	C26-C39	1.49(3)
C24-C25	1.48(5)	C28-C34	1.69(8)
C28-C39	1.66(5)	C29-C30	1.62(3)
C29-C206	1.41(4)	C30-C31	1.54(3)

C35-C36	1.58(5)	C31-C32	1.48(3)
C36-C37	1.51(4)	C32-C33	1.49(3)
C37-C187	1.46(3)	C40-C41	1.43(3)
C183-C208	1.63(3)	C182-C209	1.46(3)
C213-C214	1.54(3)	C183-C184	1.54(3)

Table S5. Bond lengths (Å) for Cu-POM-CD

W001-O0AA	1.693(9)	W001-O19	1.882(9)
W001-O5	1.904(12)	W001-O1AA	1.928(10)
W001-O11	1.941(10)	W001-O14	2.440(9)
W00A-O52	1.683(11)	W00A-O29	1.880(10)
W00A-O24	1.903(10)	W00A-O19	1.913(10)
W00A-O6B	1.914(10)	W00A-O57	2.431(9)
W00B-O216	1.664(11)	W00B-O54	1.887(11)
W00B-O100	1.889(11)	W00B-O27	1.901(11)
W00B-O77	1.914(11)	W00B-O45	2.434(9)
W00C-O8	1.701(10)	W00C-O1AA	1.884(11)
W00C-O29	1.913(10)	W00C-O49	1.922(10)
W00C-O30	1.945(10)	W00C-O28	2.436(9)
W002-O7	1.684(9)	W002-O34	1.889(9)
W002-O96	1.898(9)	W002-O9	1.913(10)
W002-O49	1.920(10)	W002-O28	2.451(9)
W003-O66	1.691(11)	W003-O42	1.878(9)
W003-O34	1.897(10)	W003-O18	1.907(10)
W003-O77	1.928(10)	W003-O45	2.424(10)
W004-O91A	1.704(9)	W004-O3	1.883(10)
W004-O27	1.884(12)	W004-O91B	1.906(10)
W004-O6B	1.936(10)	W004-O57	2.445(8)
W005-O2AA	1.681(11)	W005-O71	1.893(9)
W005-O30	1.902(10)	W005-O21	1.927(10)
W005-O9	1.928(10)	W005-O28	2.441(9)
W006-O4	1.697(11)	W006-O100	1.895(10)
W006-O3	1.919(10)	W006-O62	1.924(11)
W006-O5	1.949(12)	W006-O14	2.432(9)
W007-O50	1.668(11)	W007-O15	1.885(11)
W007-O71	1.899(10)	W007-O91B	1.913(10)
W007-O24	1.925(10)	W007-O57	2.430(9)
W008-O36	1.675(10)	W008-O96	1.880(10)
W008-O11	1.903(10)	W008-O42	1.917(9)
W008-O62	1.930(10)	W008-O14	2.434(10)
W009-O6A	1.692(9)	W009-O21	1.866(10)
W009-O15	1.904(11)	W009-O18	1.906(11)

W009-O54	1.927(11)	W009-O45	2.438(9)
Cu1-O93	2.097(11)	Cu1-O217	2.149(17)
P2-O28	1.525(9)	P2-O57	1.534(9)
P2-O14	1.535(9)	P2-O45	1.543(9)
O1-C209	1.38(2)	O1-C17	1.39(3)
O2-C35	1.39(2)	O2-C213	1.48(2)
O6-C23	1.32(3)	O10-C2	1.45(2)
O90-C21	1.31(4)	O90-C24A	1.33(4)
O90-C24B	1.85(4)	O92-C35	1.39(2)
O92-C31	1.43(2)	O94-C7	1.37(2)
O94-C11	1.51(2)	O95-C6	1.421(18)
O95-C187	1.482(19)	O97-C13	1.39(2)
O97-C183	1.39(3)	O98-C185	1.34(2)
O98-C184	1.47(2)	O101-C39B	1.31(4)
O101-C39A	1.47(3)	O101-C206	1.57(3)
O102-C182	1.38(3)	O105-C6	1.415(19)
O105-C4	1.42(2)	O106-C7	1.41(2)
O106-C3	1.42(2)	O107-C13	1.423(18)
O107-C10	1.464(19)	O115-C14	1.42(2)
O116-C12	1.40(3)	O117-C16	1.47(2)
O121-C36	1.42(3)	O131-C20	1.37(3)
O131-C185	1.54(3)	O133-C18	1.49(3)
O144-C214	1.41(3)	O147-C19	1.34(3)
O148-C41	1.44(4)	O149-C8	1.39(3)
O152-C9	1.44(2)	O154-C1	1.42(3)
O155-C5	1.39(3)	O164-C15	1.42(2)
O166-C208	1.38(3)	O210-C209	1.42(3)
O210-C40	1.54(4)	O212-C37	1.45(3)
C1-C2	1.51(3)	C1-C6	1.53(2)
C7-C8	1.54(3)	C2-C3	1.53(2)
C8-C9	1.54(3)	C3-C4	1.52(2)
C9-C10	1.54(3)	C4-C5	1.49(3)
C10-C11	1.58(2)	C16-C17	1.56(3)
C11-C12	1.53(3)	C17-C20	1.65(3)
C13-C14	1.54(2)	C18-C185	1.65(3)
C14-C15	1.49(3)	C19-C20	1.57(3)
C15-C184	1.53(3)	C21-C23	1.57(3)
C16-C18	1.40(3)	C31-C32	1.55(3)
C21-C40	1.59(4)	C30-O114	1.43(2)
C23-C182	1.64(3)	C29-C206	1.48(3)
C35-C36	1.58(3)	C206-O99	1.43(2)
C36-C37	1.44(3)	O99-C32	1.46(2)
C37-C187	1.47(2)	C39A-C28	1.47(4)

C31-C30	1.52(2)	C26A-C25A	1.60(3)
C30-C29	1.59(3)	C25A-O14A	1.42(3)
C29-O138	1.41(2)	C39B-C26B	1.53(3)
C32-C33	1.46(3)	C26B-O15B	1.39(3)
C33-O113	1.43(2)	C25B-C24B	1.49(4)
C39A-C26A	1.53(3)	C24B-O21B	1.46(3)
C26A-O15A	1.42(3)	O21B-C28	1.61(4)
C25A-C24A	1.51(3)	C34-O173	1.36(7)
C24A-O21A	1.45(3)	C183-C208	1.55(3)
O21A-C28	1.58(4)	C187-C213	1.39(3)
C26B-C25B	1.60(3)	C40-C41	1.38(3)
C25B-O14B	1.42(3)	C182-C209	1.42(3)
C28-C34	1.47(7)	C183-C184	1.53(2)